Supporting Information for

Microstructure Parameters-Dependent Non-Collinear Magnetic Structure in Scandium-Doped M-Type Hexaferrite Nanocrystal

Qiankun Qin[1], Afei Ding[1], WL Qubie[1], Pushpendra Kumar[2], Shixin Hu[1], Tianyang Yao[1], Junli Zhang[1*]

[1]School of Physical Science and Technology, Lanzhou University, Lanzhou 730000, P. R. China

[2]School of Physical Sciences, Jawaharlal Nehru University, New Delhi, 110067, India

* Corresponding authors: E-mail: zhangjl@lzu.edu.cn (Junli Zhang)

Morphology and crystal Structure

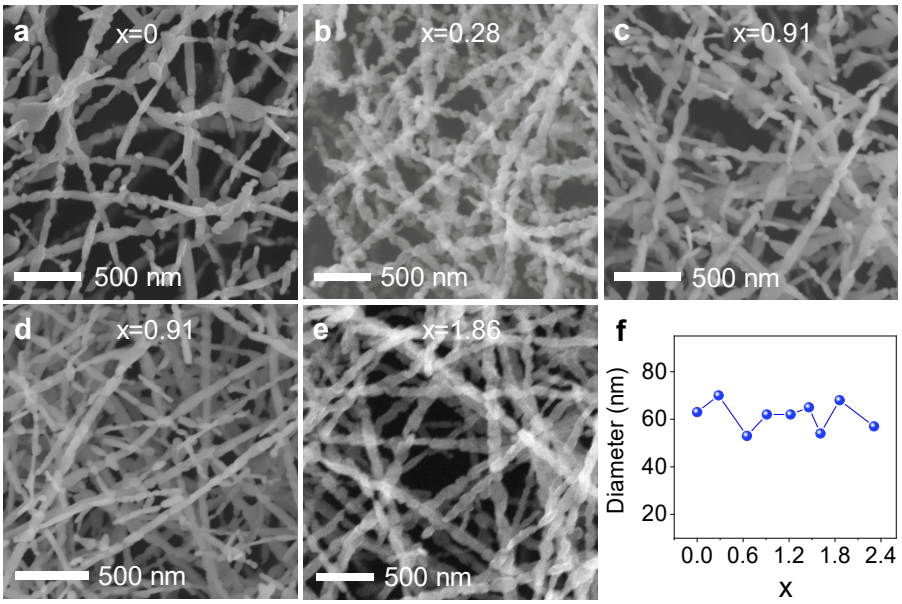

Figure S1. Morphology of $BaFe_{12-x}Sc_xO_{19}$ ($0 \leq X \leq 3.47$) nanofibers. (a-e) SEM images of $BaFe_{12-x}Sc_xO_{19}$ nanofibers with x=0, 0.28, 0.91, 1.61, 1.86 respectively. (f) Line graph of the average diameter acquired using the Nano Measure software.

$BaFe_{12-x}Sc_xO_{19}$ nanofibers with different Sc concentration nanofibers were systematically studied. Figure S1a-e shows representative SEM images of $BaFe_{12-x}Sc_xO_{19}$ (x=0, 0.28, 0.65, 0.91, 1.22, 1.46, 1.61, 1.86, 2.31, 3.04). It is clearly seen that nanofibers consist of single nanoparticles arranged in a chain-like manner along the axial direction. The average diameter is approximately 60 nm as shown in Figure S1f. Note that the chemical composition of Ba: Fe: Sc of BaFe12-xScxO19 nanofibers is confirmed by the EDX spectra (Figure S2), and the Fe concentration of all samples was demonstrated to deviate from the nominal composition of raw materials.

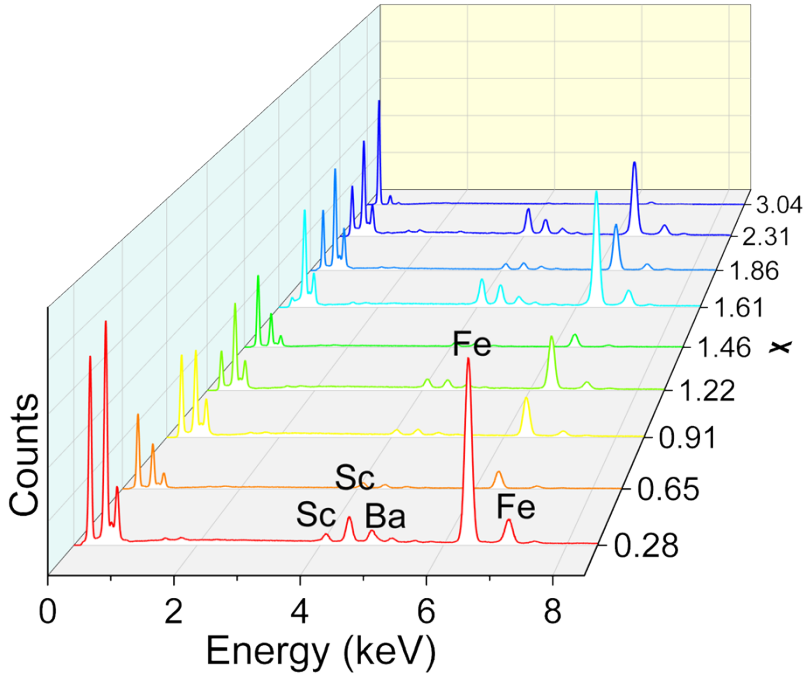

Figure S2. EDX patterns of prepared $BaFe_{12-x}Sc_xO_{19}$ ($0 \leq x \leq 3.04$) nanofibers.

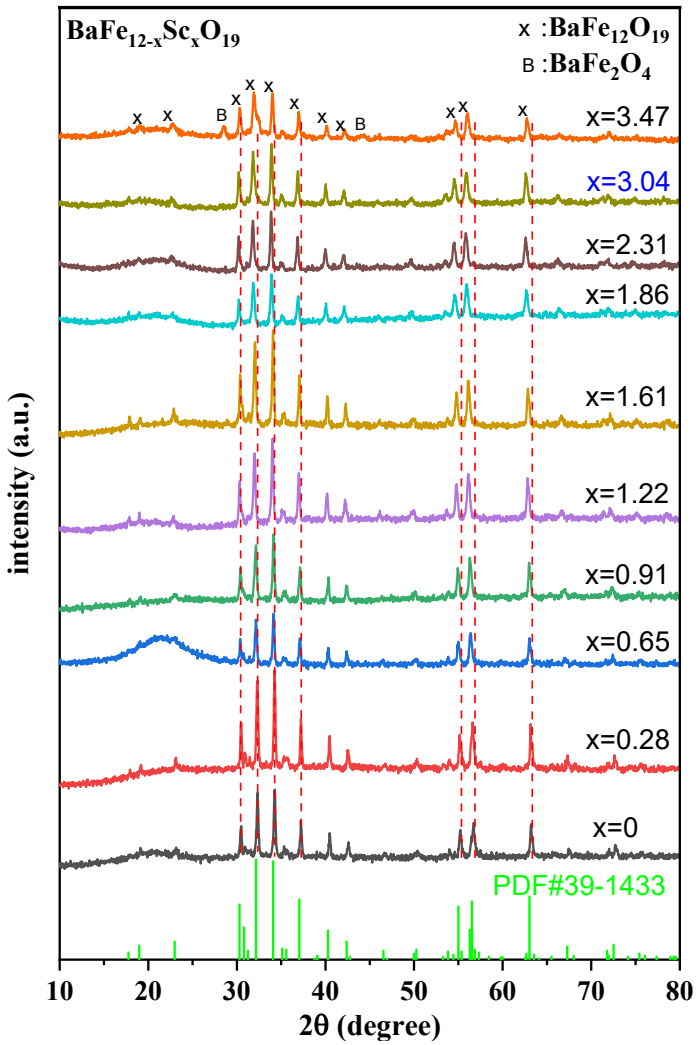

Figure S3. Room temperature X-ray diffraction patterns of $BaFe_{12-x}Sc_xO_{19}$ ($0 \leq x \leq 3.47$) nanofibers.

The XRD pattern of the $BaFe_{12-x}Sc_xO_{19}$ nanofibers indicates a *hcp* structure with *P63/mmc* space group, which is well maintained with increasing Sc content up to 3.04 (Figure S3). The diffraction peaks characteristic of M-type barium ferrite exhibits a gradual leftward shift with increasing Sc concentration, signifying an expansion of the lattice. This shift is attributed to the larger ionic radius of Sc^{3+} compared to Fe^{3+}. As the value of x increments from 0 to 3.04, this shift is approximately 0.4° to the left. Note that, the $BaFe_2O_4$ impurity spinel phase was found as doping content increased to 3.47, indicating 3.04 is an upper limit for the Sc concentration. This can be attributed to hexagonal lattice expansion and chemical potential variation of the *hcp* structure.

Figure S4. (a)-(d) Locally enlarge HAADF-TEM image and ABF-TEM image, and line intensity profiles for the atomic columns respectively at 4f_1 and 12k sites $BaFe_{12}O_{19}$ of $BaFe_{11.39}Sc_{1.61}O_{19}$. (e)-(f) Theoretical high-resolution HAADF-TEM images along the [110] zone axis of the $BaFe_{12-x}Sc_xO_{19}$, and line intensity profiles for the atomic columns at 4f_1 and 12k sites.

Table S1. Detailed refinement parameters including the substituted amount of Fe^{3+} by Sc^{3+} at different sites (2*a*, 4f_2, 2*b*), and lattice-parameter values (*a*, *c*, and *c*/*a*) with different Sc-substitution amounts.

x	2*a*	2*b*	4f_2	*a* (Å)	*c* (Å)	*c*/*a*
0	0	0	0	5.892	23.204	3.938
0.28	0.21	0	0.07	5.901	23.279	3.945
0.91	0.40	0.12	0.39	5.917	23.439	3.961
1.46	0.46	0.27	0.73	5.927	23.532	3.971
1.61	0.48	0.32	0.81	5.931	23.561	3.973
1.86	0.52	0.98	0.36	5.944	23.651	3.979

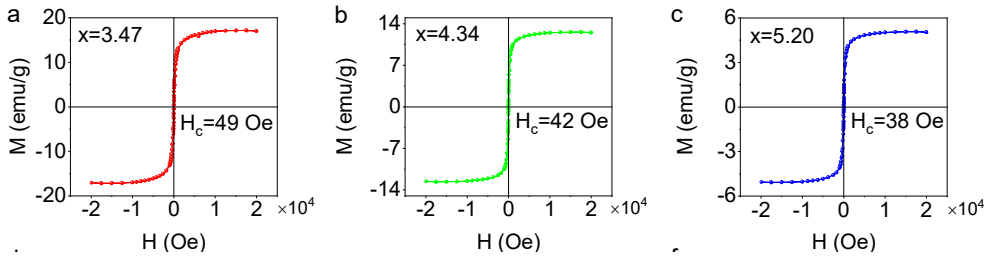

Figure S5. Room temperature hysteresis loops of $BaFe_{12-x}Sc_xO_{19}$ ($3.47 \leq x \leq 12$) nanofibers.

The presence of $BaFe_2O_4$ and other impurity phases is likely to attenuate the saturation magnetization and coercivity of our specimens when x further increased from 3.47 to 5.20, as indicated by Figure S5.

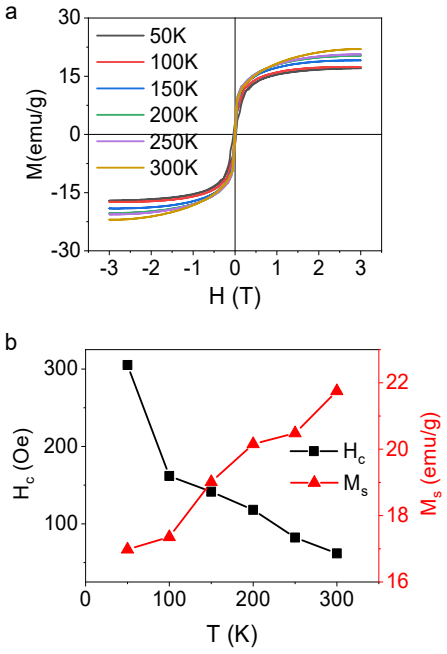

Figure S6. (a) Hysteresis loops of $BaFe_{12-x}Sc_xO_{19}$ with x=3.04 (b) Temperature dependence of coercivity and saturation magnetization.

Table S2. Detailed refinement parameters of $BaFe_{12}O_{19}$.

Sublattice	Coordination	B_{hf} (T)	IS (mm/s)	QS (mm/s)
$4f_2$ (Fe4)	octahedral	51.0(1)	0.34(1)	0.10(2)
2*a* (Fe1)	octahedral	48.7(2)	0.27(3)	0.33(5)
$4f_1$ (Fe3)	tetrahedral	48.2(4)	0.31(5)	0.03(9)
12*k* (Fe5)	octahedral	41.5(4)	0.30(1)	0.41(1)
2*b* (Fe2)	bi-pyramidal	38.7(3)	0.48(4)	2.15(7)

Table S3. Detailed refinement parameters of $BaFe_{12-x}Sc_xO_{19}$ with x=1.61 and 1.86.

x value	B_{hf} (T)	IS (mm/s)	QS (mm/s)
1.61	29.1(0)	0.37 (0)	0.18(8)
1.86	23.7(9)	0.39(3)	0.16(3)